THE JOURNAL OF PHYSICAL CHEMISTRY C

Article

pubs.acs.org/JPCC

Nanoparticle Silver Catalysts That Show Enhanced Activity for Carbon Dioxide Electrolysis

Amin Salehi-Khojin,*[,†,‡] Huei-Ru Molly Jhong,[§] Brian A. Rosen,[†,§] Wei Zhu,[†] Sichao Ma,[§] Paul J. A. Kenis,[§] and Richard I. Masel*[,†]

[†]Dioxide Materials, 60 Hazelwood Drive, Champaign, Illinois 61820, United States

[‡]Department of Mechanical & Industrial Engineering, University of Illinois−Chicago, 842 West Taylor Street, Chicago, Illinois 60607, United States

[§]Department of Chemical & Biomolecular Engineering, University of Illinois Urbana−Champaign, 600 South Mathews Avenue, Urbana, Illinois 61801, United States

Supporting Information

ABSTRACT: Electrochemical conversion of CO_2 has been proposed both as a way to reduce CO_2 emissions and as a source of renewable fuels and chemicals, but conversion rates need improvement before the process will be practical. In this article, we show that the rate of CO_2 conversion per unit surface area is about 10 times higher on 5 nm silver nanoparticles than on bulk silver even though measurements on single crystal catalysts show much smaller variations in rate. The enhancement disappears on 1 nm particles. We attribute this effect to a volcano effect associated with changes of the binding energy of key intermediates as the particle size decreases. These results demonstrate that nanoparticle catalysts have unique properties for CO_2 conversion.

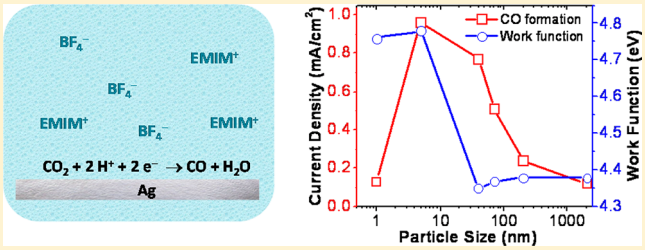

INTRODUCTION

The discovery and development of efficient catalysts for CO_2 electroreduction is one of the grand challenges identified in the Department of Energy (DOE) report, Catalysis for Energy.[1] If electrochemical reduction of CO_2 is to become feasible, catalysts are needed that exhibit both high energetic efficiency and high conversion rates.[2] Recently, we discovered that the combination of two catalysts, a silver metal and ionic liquid 1-ethyl-3-methylimidazolium tetrafluoroborate (EMIM-BF_4) would lower the overpotential for CO_2 reduction by almost a volt.[3,4] Unfortunately, rates were lower than needed. The objective of this article is to determine whether the rate would be enhanced by lowering the particle size of the silver catalysts. A previous paper[5] reported a higher rate for CO_2 conversion on Ag(110) than on Ag(111) or Ag(100), but the effect was not large enough to have a significant effect on practical supported catalysts. Small variations are also seen on platinum single crystals,[6,7] but again, the effects are too small to have a significant effect on practical catalysts. Still, previous workers had shown that gold nanoparticles have unique properties for a number of reactions. Therefore, we decided to determine whether silver nanoparticles have unique properties for CO_2 conversion in ionic liquids.

EXPERIMENTAL SECTION

The 5 nm catalyst was a custom-made sample from a local supplier. The 1 nm sample was prepared from Mesosilver manufactured by Colloids For Life. The 200, 70, and 40 nm samples were purchased from Sigma Aldrich. (Sigma-Aldrich labels its samples <500, <100, and 40 nm.) The nomenclature of 200, 70, 40, 5, and 1 nm represents the actual average particle size of the samples as measured by dynamic light scattering and confirmed by transmission electron microscopy (TEM).

In the electrochemical experiments, each catalyst sample was deposited onto a clean silver substrate, baked to remove organic impurities, and then soaked in acid or ionic liquid solution to remove metallic impurities. X-ray photoelectron spectroscopy (XPS) of similar samples on a silicon substrate showed the samples to be clean, except for small amounts of carbon and oxygen from the vacuum system. The samples were loaded into a standard 3 electrode cell for the measurements. In each plot, the current was normalized by the electrochemical surface area of each electrode, measured by underpotential deposition lead stripping. Details of all procedures are given in the Supporting Information.

The ultraviolet photoelectron spectroscopy (UPS) data was taken after depositing the catalyst materials onto silicon substrates heating and soaking in acid, using a Physical Electronics PHI 5400 photoelectron spectrometer that uses HeI (21.2 eV) ultraviolet radiation and a pass energy of 8.95 eV. To separate the signal arising from secondary electron

Received: November 5, 2012
Revised: December 23, 2012
Published: December 24, 2012

   dx.doi.org/10.1021/jp310509z | J. Phys. Chem. C 2013, 117, 1627−1632

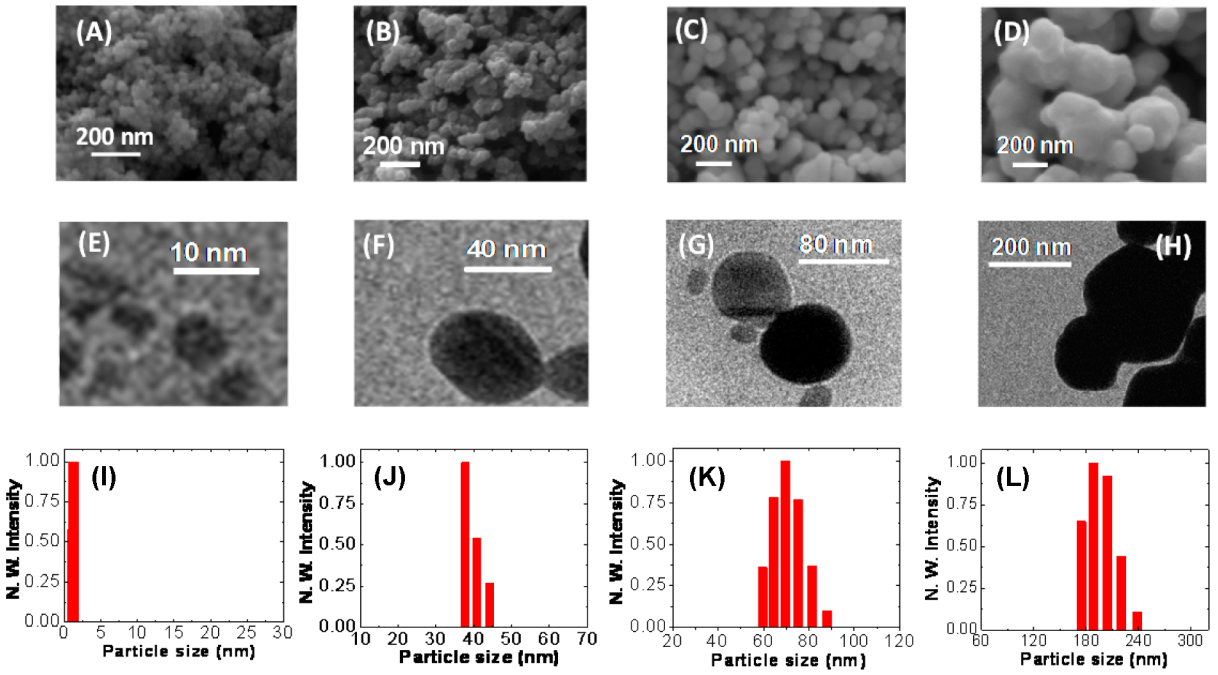

Figure 1. (A–D) SEM images of 1, 5, 70, and 200 nm silver nanoparticles, respectively. (E–H) TEM images of 5, 40, 70, and 200 nm silver nanoparticles, respectively. (I–L) DLS results for 1, 40, 70, and 200 nm particles, respectively.

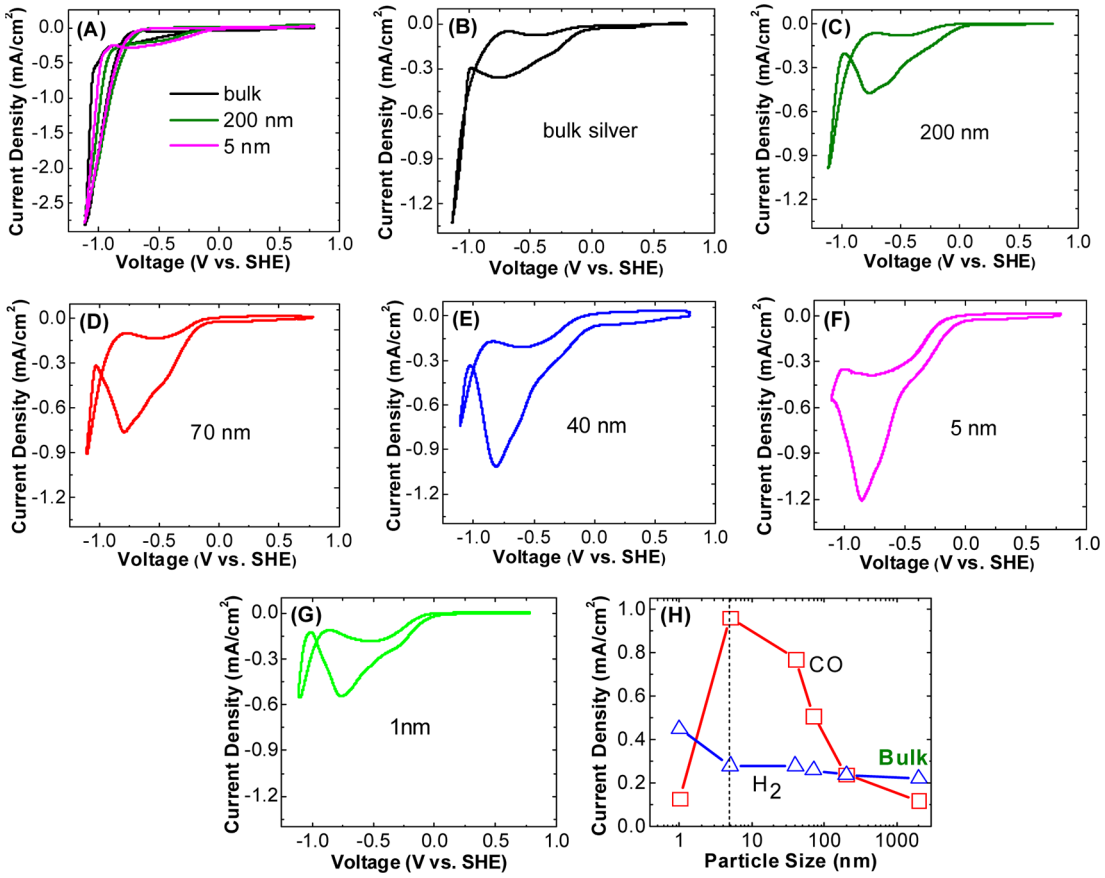

Figure 2. (A) Cyclic voltammetry with argon in EMIM-BF_4 on bulk and 200 and 5 nm silver nanoparticle catalysts (see Figure S3, Supporting Information, for the expanded results). (B–G) cyclic voltammetry with CO_2 in EMIM-BF_4 on bulk and 200, 70, 40, 5, and 1 nm silver nanoparticle catalysts, respectively. (H) Current density for CO and H_2 formation as a function of particle size (the numbers of current density for CO and H_2 formation are obtained from the differences in the current density with CO_2 (from B–G) and Argon (from A) at −0.75 V vs SHE and −1.14 V vs SHE, respectively. The maximum current density for the CO peak occurs at 5 nm.

dx.doi.org/10.1021/jp310509z | J. Phys. Chem. C 2013, 117, 1627–1632

emission from the detector from the secondary electron emission from the sample, a −9 V bias was applied to the sample using a battery. The reported binding energies are the measured binding energy plus the 9 V.

In the flow apparatus described previously,[3] catalysts were painted onto carbon paper and mounted in a 2 compartment cell. Dried ionic liquid flowed through the cathode compartment, while 0.5 M sulfuric acid flowed into the anode. Voltage was applied to the cell, and the CO and hydrogen production were measured with a gas chromatograph.

RESULTS AND DISCUSSION

In this study, we used different silver nanoparticle sizes ranging from 1 to 200 nm. Figure 1A−H shows the scanning electron microscopy (SEM) and TEM images of the nanoparticles. Figure 1I−L shows the results of dynamic light scattering (DLS) analysis which are in a good agreement with TEM results. To investigate the electronic properties of silver nanoparticles, XPS was carried out. Prior to measurements, the samples were immersed in 0.1 M sulfuric acid overnight and rinsed with DI water to remove impurities. XPS spectra were collected using a Kratos Axis ULTRA X-ray photoelectron spectrometer with monochromatic Al Kα excitation, 120 W (120 kV and 10 mA). Survey spectra were collected at a pass energy of 160 eV, and high-resolution spectra were collected using a pass energy of 40 eV. XPS results show that samples are clean, except for small amounts of carbon and oxygen from the vacuum system.

Figure 2 shows the result of a cyclic voltammetry (CV) experiment where nanoparticle silver was coated onto a silver rotating disk electrode, the electrode was loaded into an EMIM-BF_4 solution containing about 75 ppm of water, the sample was rotated at 1000 rpm, and the potential was cycled from −1.14 to 0.77 V with respect to SHE (see Supporting Information for experimental details). Figure 2a shows how the CV of water varies with particle size under the conditions of the experiment. The plot shows how the current per unit surface area (i.e., the measured current divided by the measured surface area) varies with the particle size. Notice that all of the curves lie on top of each other, demonstrating that the rate per unit surface area of water electrolysis to produce hydrogen is independent of particle size, as would be expected from previous literature.[8] The rate in an electrochemical reaction is proportional to the current in the reaction. For example, two electrons are needed for the reaction:

$$CO_2(g) + 2H^+(l) + 2e^- \rightarrow CO(g) + H_2O(l) \quad (1)$$

Thus, the rate of reaction in moles per second is 1/2 the current divided by a constant *F*, called Faraday's constant.

Figure 2 also shows similar experiments except that we bubbled CO_2 through the solution. In this case, we observe a peak centered at about −0.75 V vs SHE that is not seen in the absence of CO_2. This peak is associated with CO_2 conversion. Notice that the peak grows as the particle size decreases from 200 to 5 nm, and then shrinks again as the particle size decreases to 1 nm. In other words, the results in Figure 2B−G shows that the rate of CO_2 electrolysis depends strongly on the particle size.

Figure 2h illustrates the effect more clearly. Specifically, the peak current densities for CO formation (i.e., current densities at −0.75 V vs SHE) in Figure 2B−G were plotted with respect to particle size to quantitatively show how the rate of CO_2 reduction changes as a function of particle size. Notice that the rate of CO_2 electrolysis is about a factor of 10 higher on 5 nm silver particles than on bulk silver surfaces or on catalysts composed of 1 nm particles. Clearly, this is a significant effect.

Figure 3A,B shows steady-state data taken using the flow apparatus described previously.[3,9] Briefly, the dual-electrolyte

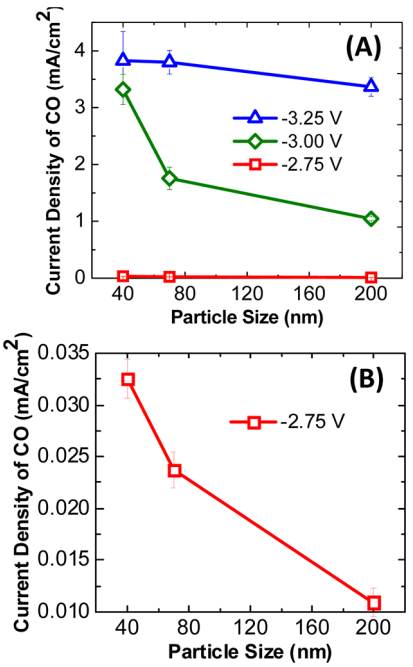

Figure 3. (A) Current density of CO as a function of silver particle size at different cell voltage (−2.75, 3.00, and 3.25 V) measured in a flow cell. (B) Data for −2.75 V on an expanded scale. These data were taken with EMIM solutions containing about 75 μM water. Previous work[3] used 88% water on the cathode, resulting in much higher currents.

electrochemical reactor (Figure 3C) used in this study consists of two 1.5 mm thick poly(methyl methacrylate) (PMMA) sheets with 0.5 cm wide by 2.0 cm long channels to provide the electrolyte flow channels for the catholyte (liquid stream in contact with the cathode; pure EMIM BF_4) and analyte (liquid stream in contact with the anode; 0.5 M sulfuric acid). Between the two electrolyte channels was a 0.8 cm wide and 2.5 cm long piece of Nafion 212 membrane (DuPont) used to separate the catholyte and anolyte while maintaining ionic conductivity. The cathode and anode that were made of gas diffusion electrodes (GDEs) were put on each PMMA sheet. Each electrode was backed by aluminum current collectors. The aluminum current collector that backed the cathode also served as a gas flow chamber to supply CO_2, while the anode was open to the atmosphere for oxygen to escape. At cell voltages of 3 V or less, the CO current increases by a factor of 3 in changing from 200 to 40 nm particles. This is very similar to the change seen in Figure 2h. The particle size dependence disappears at higher applied voltages, however.

It is interesting to compare the results in Figures 2 and 3 to previous results for CO_2 conversion on single crystal catalysts. Hoshi et al.[5] previously examined CO_2 conversion on Ag(111), Ag(100), and Ag(110) and found that the rate of CO_2 reduction was about a factor of 2 higher on Ag(110) than on Ag(111) or Ag(100). If one assumes that the flat surface was mainly (111) or (100) orientated, while (110) facets and

dx.doi.org/10.1021/jp310509z | J. Phys. Chem. C 2013, 117, 1627−1632

related steps cover that 20% of the surface of the 5 nm particle, then on the basis of the single crystal results, one would only expect the rate to go up by about 20%, i.e., 20%*(2−1). By comparison, Figure 2 shows an order of magnitude change in rate. Further, the 1 nm particles are the most irregular, yet they show a decreased activity compared to the single crystal results.[5] Thus, the nanoparticle catalysts used here clearly exhibit much different variations in rate as a function of structure than what would be expected from the single crystal results reported previously.

The explanation for these different effects is not obvious. Variations in rate with particle size can be caused by (i) variation in the number of step sites, kink sites, and other special geometries with particle size, (ii) variation in the electronic structure or work function of the particles with particle size, or (iii) variation in the binding energy of key intermediates with particle size.[10] Experimentally, we observe much larger variations in rate with particle size than was expected from work on single crystals;[5,7] so, variations in the concentration of steps, kinks, and other structures do not seem to explain our data.

We have considered changes in rate due to variations in the bulk electronic properties of the particles such as the work function or d-band position, but our UPS data (see Supporting Information for details of experiments) shown in Figure 4

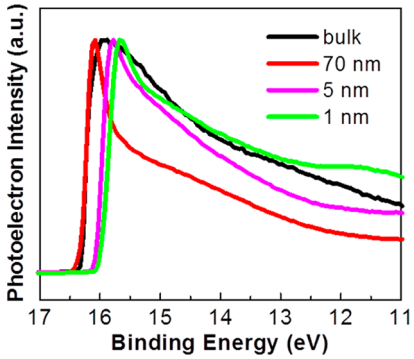

Figure 4. UPS spectra of 1, 5, and 70 nm of clean silver nanoparticles as well as of bulk silver. To allow for easy comparison of curve shape, the data has been rescaled on the *Y*-axis so that the maximum intensities of all the UPS peaks are the same.

indicate that the variations in the work function and the position of the center of the d-bands is insufficient to explain the observed variations in rate. Notice that the general shape of the UPS spectrum of the particles does not vary significantly with particle size at particle sizes down to 5 nm. Importantly, the center of the d-band is not shifting significantly with particle size. We do observe variations in the work function of the particles with particle size as indicated in Table 1. Still, the work function is almost the same in bulk samples and in 40 nm particles, even though the rate varies significantly. Similarly, the measured work function is almost the same on 5 and 1 nm particles, even though the rate changes significantly. In each of these two cases, the variations in work function with particle size are smaller than the variations in work function with the crystal face reported previously.[11,12] Thus, the variations in the work function and the electronic structure of our particles does not explain why we observe variations in rate with particle size that are larger than those seen on single crystal catalysts.

Table 1. Measured Work Functions of the Particles

particle size	measured work function (eV)	work function variation expected from Wood's model[18] (eV)
bulk	4.38 ± 0.022	4.37
70 nm	4.38 ± 0.023	4.38
40 nm	4.35 ± 0.026	4.38
5 nm	4.78 ± 0.019	4.48
1 nm	4.76 ± 0.050	4.91

That leaves variations in the binding energy of intermediates as the explanation for the observed variation in rate. To see if the binding energy of intermediates would vary with particle size, we performed cyclic voltammetry (CV) to determine the binding energy of hydroxyls and sulfates (or bisulfates) as a function of particle size. Specifically, the overpotential of hydroxyl/sulfate adsorption is considered a measure of binding strength of intermediates on silver nanoparticles; smaller overpotential indicates larger binding energy (stronger binding) of intermediates. Figure 5 shows voltammograms of the sulfate

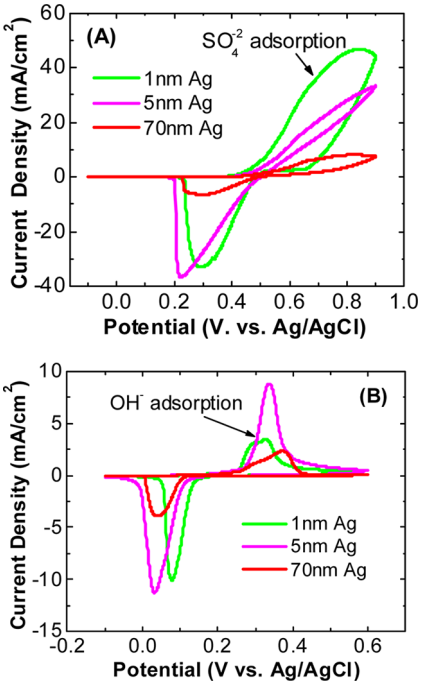

Figure 5. Adsorption and desorption of (A) sulfate and (B) hydroxide on 1, 5, and 70 nm silver nanoparticles. The overpotential for both hydroxide and sulfate goes down as the particle size decreases.

and hydroxyl adsorption and desorption peaks on different diameter silver particles in 0.1 M sulfuric acid or 0.1 M NaOH. In this experiment, hydroxide adsorption scans were swept between −0.1 and 0.6 V and sulfate scans between −0.1 and 0.9 V vs Ag/AgCl. All scans were taken at 10 mV/s. The current was normalized by the electrochemical surface area of each electrode, measured by underpotential deposition lead stripping.

For the hydroxide peaks, we observe a shift in the overpotential required to drive the adsorption and desorption. At a current density of +2.5 mA/cm^2, the overpotential required to drive the adsorption at this rate is lowest on the 1 nm silver particles and increases by about 100 mV with increasing particle size. Desorption of the hydroxide anion at the same rate (−2.5 mA/cm^2) follows the same trend. The

dx.doi.org/10.1021/jp310509z | J. Phys. Chem. C 2013, 117, 1627−1632

overpotential is lowest using the 1 nm silver particles and increases with increasing particle size. This was also observed for the adsorption and desorption of the sulfate anion. This implies that the binding energy of sulfates and hydroxyls varies significantly with particle size, with the smallest particles showing higher binding than bulk samples. Importantly, this effect is larger than that observed in single crystals.[13−16] In summary, these data suggest that differences in the binding energy of intermediates with particles of different size is large enough to explain why we observe larger increases in rate than has been observed in single crystals.

It is interesting to ask how the variations in binding energy could cause changes in rate. Assume for the moment that the conversion of CO_2 to CO under acidic conditions in the presence of $EMIM^+$ (EMIM-BF_4 is acidic) followed the mechanism proposed by Rosen et al.:[3,4]

$$EMIM^+(l) + CO_2(g) + e^- \rightarrow complex^-_{(ad)}(l) \quad (2)$$

$$H^+(l) + complex^-_{(ad)}(l) \rightarrow CO(g) + OH^-_{(ad)} + EMIM^+(l) \quad (3)$$

$$OH^-_{(ad)} + H^+(l) + e^- \rightarrow H_2O(l) \quad (4)$$

If the binding energy of the intermediates increased with shrinking particle size, the thermodynamic driving force for reactions 2 and 3 should increase, while the thermodynamic driving force for reaction 4 should decrease. Therefore, one would expect the rate of reactions 2 and 3 to increase, and the rate of reaction 4 to decrease. In our previous papers,[3,4] we suggested that, during CO_2 conversion on 100−200 nm silver particles, reactions 2 and 3 are rate determining. In that case, one could increase the rate by increasing the binding energy of intermediates by, for example, making the particle sizes smaller. However, if we increased the binding energy of the intermediates enough, reaction 4 would become rate determining. In that case, the rate of reaction would decrease since the OH cannot be rapidly removed from the surface. Consequently, one would expect classic volcano behavior as seen in Figure 2h.

This model would also explain why the variations in rate with particle size are larger than those seen with single crystals. Previous data with single crystal catalysts show that sulfate[13,14] and hydroxyl binding[15,16] is only weakly affected by crystal face. Sulfate binds more strongly on Ag(111) than on Ag(100) or Ag(110),[13,14] while the literature disagrees whether the (111) or (100) face of silver binds oxygen most strongly. In all cases, the effects are 50 mV or less. By comparison, we observe almost 100 mV variations in binding energy. Thus, we observe larger variations in rate with nanoparticles than with single crystals because the binding energy of intermediates varies more strongly with geometry on nanoparticles than on single crystals.

Of course, we still have to explain why the variations in binding energy occur. One needs calculations to do so, and we have not done them yet. Still, recent calculations of Pozen et al.[17] show that the binding energy of ethylene varies more strongly on silver nanoparticles than expected from data on single crystal samples. Thus, there is precedent in the literature.

CONCLUSIONS

In summary, we have studied the effect of Ag nanoparticle size on its catalytic performance in the conversion of CO_2 into CO. We found that the catalytic activity increases with decreasing particle size until a certain particle size, here, 5 nm, and that the activity drops when going to even smaller nanoparticle size (1 nm). Through UPS measurements (work function) and further electrochemical analysis (binding strengths), we were able to conclude that some reaction intermediates bind too strongly to the nanoparticles once they are too small, here, <5 nm. We expect that other metal nanoparticles will exhibit similar size-dependent effects, but further studies would be needed to confirm.

ASSOCIATED CONTENT

Supporting Information

Details of the structural characterizations, electronic characterizations, and electrochemical experiments. This material is available free of charge via the Internet at http://pubs.acs.org.

AUTHOR INFORMATION

Corresponding Author

*E-mail: salehikh@uic.edu (A.S.-K.); rich.masel@dioxidematerials.com (R.I.M.).

Notes

The authors declare the following competing financial interest(s): RM is the founder and principal owner of Dioxide Materials, a company that is working to commercialize the findings in this paper. RM and AS submitted a US Patent Application number 13/445,887 Catalysts for CO2 conversion. RM, BR and WZ have related patents. The other authors declare no competing financial interests.

ACKNOWLEDGMENTS

This work was supported in part by the Department of Energy under grant DE-SC0004453 and by Dioxide Materials. Any opinions, findings, and conclusions or recommendations expressed in this article are those of the authors and do not necessarily reflect the views of the Department of Energy. This work was carried out in part in the Frederick Seitz Materials Research Laboratory Central Facilities, University of Illinois. We wish to acknowledge Rick Haasch for his assistance with the UPS measurements.

REFERENCES

(1) Bell, A. T. *Basic Research Needs: Catalysis For Energy*; US Department of Energy: Washington, DC, 2008.
(2) Whipple, D. T.; Kenis, P. J. A. *J. Phys. Chem. Lett.* **2010**, *1* (24), 3451−3458.
(3) Rosen, B. A.; Salehi-Khojin, A.; Thorson, M. R.; Zhu, W.; Whipple, D. T.; Kenis, P. J. A.; Masel, R. I. *Science* **2011**, *334*, 643−644.
(4) Rosen, B. A.; Haan, J. L.; Mukherjee, P.; Braunschweig, B.; Zhu, W.; Salehi-Khojin, A.; Dlott, D. D.; Masel, R. I. *J. Phys. Chem. C* **2012**, *116* (29), 15307−15312.
(5) Hoshi, N.; Kato, M.; Hori, Y. *J. Electroanal. Chem.* **1997**, *440* (1−2), 283−286.
(6) Hoshi, N.; Hori, Y. *Electrochim. Acta* **2000**, *45* (25−26), 4263−4270.
(7) Hoshi, N.; Sato, E.; Hori, Y. *J. Electroanal. Chem.* **2003**, *540* (0), 105−110.
(8) Koper, M. T. M. *Nanoscale* **2011**, *3* (5), 2054−2073.
(9) Whipple, D. T.; Finke, E. C.; Kenis, P. J. A. *Electrochem. Solid-State Lett.* **2010**, *13* (9), B109−B111.
(10) Masel, R. I. *Principles of Adsorption and Reaction on Solid Surfaces*; Wiley: New York, 1996.

(11) Dweydari, A. W.; Mee, C. H. B. *Phys. Status Solidi A* **1975**, *27* (1), 223−230.
(12) Chelvayohan, M.; Mee, C. H. B. *J. Phys. C* **1982**, *15* (10), 2305.
(13) Smoliński, S.; Zelenay, P.; Sobkowski, J. *J. Electroanal. Chem.* **1998**, *442* (1−2), 41−47.
(14) Sobkowski, J.; Smolinski, S.; Zelenay, P. *Colloids Surf., A* **1998**, *134*, 39−45.
(15) Blizanac, B. B.; Ross, P. N.; Markovic, N. M. *J. Phys. Chem. B* **2006**, *110* (10), 4735−4741.
(16) Zwetanova, A.; Jüttner, K. *J. Electroanal. Chem. Interfacial Electrochem.* **1981**, *119* (1), 149−164.
(17) Pozun, Z. D.; Tran, K.; Shi, A.; Smith, R. H.; Henkelman, G. *J. Phys. Chem. C* **2011**, *115* (5), 1811−1818.
(18) Wood, D. *Phys. Rev. Lett.* **1981**, *46*, 449.